Published in IEEE Sensors Journal 14, 9, 3193-2000, 2014
which should be used for any reference to this work

The Microloop-Gap Resonator: A Novel Miniaturized Microwave Cavity for Double-Resonance Rubidium Atomic Clocks

Maddalena Violetti, Matthieu Pellaton, Christoph Affolderbach, *Member, IEEE*, Francesco Merli, *Member, IEEE*, Jean-François Zürcher, Gaetano Mileti, and Anja K. Skrivervik

***Abstract*— Nowadays mobile and battery-powered applications push the need for radically miniaturized and low-power frequency standards that surpass the stability achievable with quartz oscillators. For the miniaturization of double-resonance rubidium (^{87}Rb) atomic clocks, the size reduction of the microwave cavity or resonator (MWR) to well below the wavelength of the atomic transition (6.835 GHz for ^{87}Rb) is of high interest. Here, we present a novel miniaturized MWR, the μ-LGR, for use in a miniature DR atomic clock and designed to apply a well-defined microwave field to a microfabricated Rb cell that provides the reference signal for the clock. This μ-LGR consists of a loop-gap resonator-based cavity with very compact dimensions (<0.9 cm^3). The μ-LGR meets the requirements of the application and its fabrication and assembly can be performed using repeatable and low-cost techniques. The concept of the proposed device was proven through simulations, and prototypes were successfully tested. Experimental spectroscopic evaluation shows that the μ-LGR is well-suited for use in an atomic clock. In particular, a clock short-term stability of $7 \times 10^{-12}\tau^{-1/2}$ was measured, which is better than for other clocks using microfabricated cells and competitive with stabilities of compact Rb clocks using conventional glass-blown cells.**

***Index Terms*— Microwave devices, microwave measurements, atomic measurements, spectroscopy, frequency control, metrology.**

I. Introduction

ATOMIC frequency standards (atomic clocks) provide the most stable and accurate frequency references available, by exploiting a well-defined atomic transition to steer the output frequency of a quartz oscillator [1]. Vapor-cell atomic clocks [2] are highly compact (volumes ranging from 50 cm^3 to around 2.5 dm^3) atomic clocks, that are well established devices for, e.g., synchronization in telecommunication networks [3] or as on-board clocks in satellite navigation systems [4]. The past decade has seen rapid progress in the development of vapor-cell based chip-scale atomic clocks (CSACs), achieving clock integration in volumes of a few cm^3, and a total power consumption around 100 mW [5], [6]. These CSACs show fractional frequency instabilities (Allan deviation) below 10^{-11} at timescales of one hour, i.e. several orders of magnitude better than a quartz oscillator of comparable size and power consumption. There is presently an emerging need for such radically miniaturized and low-power atomic clocks, for use in mobile and battery-powered applications such as communication and localization systems, as well as in telecommunication or power distribution networks, where atomic clocks as replacements for quartz oscillators can provide improved hold-over capabilities [7].

Most approaches to CSACs have been based on the Coherent Population Trapping scheme (CPT) [5], while the classical optical-microwave double-resonance (DR) scheme [2], [8] has been only rarely studied [8]–[10]. Nevertheless, in comparison with CPT, the DR approach has several advantages: Thanks to the absence of non-resonant laser modulation sidebands, the DC background level of the signal is reduced, which reduces the detection noise and therefore improves on the signal-to-noise ratio of the clock signal. In addition, DR allows for a ten times higher signal amplitude than CPT, while degrading the linewidth by only a factor of two. Therefore, in similar operating conditions, DR typically gives a five times better short-term stability than CPT [9].

In a DR rubidium atomic clock (see Fig. 1 for a block scheme) the microwave resonator (MWR) is used to apply a stable microwave field of well-defined geometry to the Rb atoms held in a vapor cell. For the miniaturization of the clock, the size reduction of the MWR to well below the wavelength of the atomic transition (4.3 cm for the case of the 6.835 GHz transition in ^{87}Rb) has been a long-standing issue. Solutions such as the magnetron-type MWR [11], miniature MWR using lumped LC elements [12], or slotted-tube MWR [13] were developed for Rb cells down to $\approx$1 cm size. Only a very

Manuscript received March 17, 2014; accepted May 7, 2014. Date of publication May 22, 2014; date of current version July 25, 2014. This work was supported by the Swiss National Science Foundation through the Sinergia under Grant CRSI20 122693. The associate editor coordinating the review of this paper and approving it for publication was Dr. Richard T. Kouzes.

M. Violetti, J.-F. Zürcher, and A. K. Skrivervik are with the Laboratoire d'Electromagnétisme et d'Acoustique, École Polytechnique Fédérale de Lausanne, Lausanne CH-1015, Switzerland (e-mail: maddalena.violetti@epfl.ch; jf.zurcher@epfl.ch; anja.skrivervik@epfl.ch).

M. Pellaton, C. Affolderbach, and G. Mileti are with the Laboratoire de Temps-Fréquence, Université de Neuchâtel, Neuchâtel CH-2000, Switzerland (e-mail: matthieu.pellaton@unine.ch; christoph.affolderbach@unine.ch; gaetano.mileti@unine.ch).

F. Merli was with the Laboratoire d'Electromagnétisme et d'Acoustique, École Polytechnique Fédérale de Lausanne, Lausanne CH-1015, Switzerland. He is now with Huber+Suhner AG, Herisau CH-9100, Switzerland (e-mail: francesco.merli@epfl.ch).

Color versions of one or more of the figures in this paper are available online at http://ieeexplore.ieee.org.

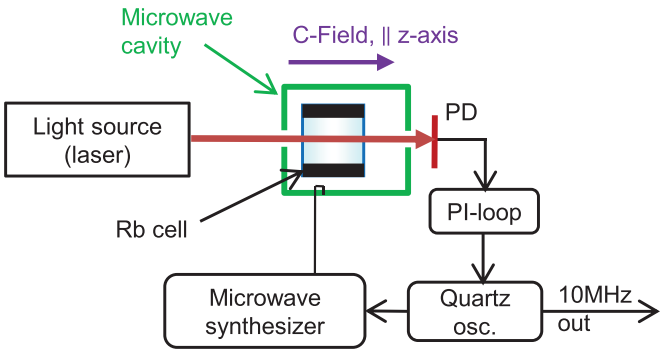

Fig. 1. Block scheme of a double-resonance Rb atomic clock.

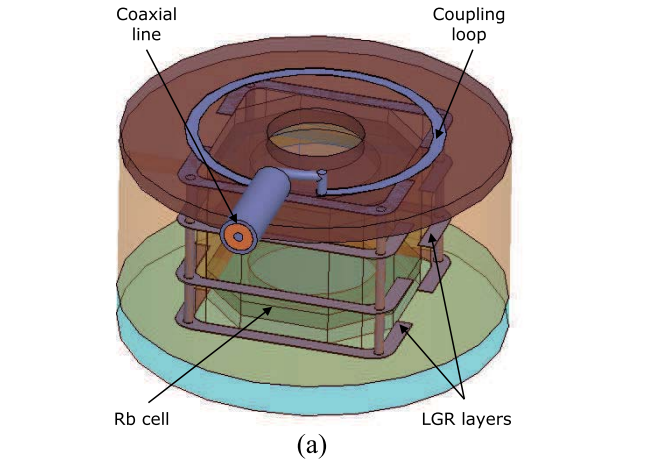

Fig. 2. (a) Cut view of the μ-LGR design. (b) Assembled test enclosure of the miniaturized cavity. (c) Fabricated μ-LGR stack with integrated Rb cell, outer diameter of the dielectric substrates is 11.0 mm.

small number of microwave structures have been reported for use with micro-fabricated cells on the scale of few millimeters, which have been based on non-resonant strip-lines or micro coupling loops [10].

In this paper we present a novel miniature MWR, the μ-LGR [14], [15], designed to apply a well-defined microwave field to a 50 mm^3 internal volume microfabricated Rb cell [16]. The aim of this study was to provide a clock short-term stability equal or below $1 \times 10^{-11}\tau^{-1/2}$ at short integrations times $\tau = 1$ s to 100 s, from a miniaturized MWR package.

The μ-LGR design is composed of a multi-layer stack of printed loop-gap resonator structures, coupled to a coaxial fed strip-line (see Fig. 2(a)). The total cavity volume is less than 0.9 cm^3. Two screws mounted into the MWR metallic enclosure and inserted into the cavity allow fine tuning of the resonant frequency (Fig. 2(b)). The enclosure has apertures at its ends to allow the laser beam to interact with the ^{87}Rb atomic vapor, which is held in a micro-fabricated cell placed in the center of the μ-LGR (Fig. 2(c)).

The loop-gap resonator approach allows the geometric field requirements for DR atomic clocks to be met (the microwave magnetic field has to be collinear with the laser beam and the applied static magnetic "C-field," i.e. along the z direction). The use of printed-circuit technology keeps the structure compact and suitable for low-cost batch fabrication using established techniques. The principle of operation was studied and optimized through software simulations that were aimed to study the influence of relevant geometrical features, the presence of the Rb cell and of the cavity apertures. Prototypes of an optimized solution were built and successfully tested. Laboratory tests proved the suitability of the proposed structure for integration in miniaturized Rb atomic clocks. First clock operation using the μ-LGR achieved short-term stabilities unmatched by other clocks with microfabricated Rb cells, demonstrating the potential of our MWR approach and similar implementations for CSAC applications as well as slightly larger but more high-performance compact Rb clocks.

II. Requirements

The homogeneity of intensity and orientation of the microwave field across the Rb vapor cell, and thus inside the MWR, are of great importance to the performance of the atomic frequency standard. The microwave magnetic field should be parallel to the direction of propagation of the laser light beam and to the direction of the C-field (both assumed to be parallel to the z-axis here, see Fig. 1), with a magnitude on the level of $\sim 10^{-8}$ Tesla.

In order to assess the degree to which the microwave magnetic field is parallel to the dc magnetic C-field, i.e. to the z-axis, we calculate the Field Orientation Factor (FOF), ξ [17]:

$$\xi = \frac{1}{V_{\text{cell}}} \frac{\int_{V_{\text{cell}}} H_z^2 dV}{\int_{V_{\text{cell}}} |\mathbf{H}|^2 dV} \tag{1}$$

This FOF gives the fraction of microwave magnetic field power (integrated over the active cell volume V) that is oriented parallel to the C-field direction, which is the component driving the desired clock transition, as will be detailed in section VI-B.

III. Proposed Solution

A. Design Concept

The general Loop-Gap Resonator (LGR), also referred to as the split ring resonator [18] or slotted tube cavity [19], can be represented, in its simplest model, by an LC circuit where the loop is an inductor and the gap is a capacitor. The electric fields are supported by the gap with the magnetic fields surrounding the loop [20]. When the dimensions of the resonator are significantly smaller than the half-wavelength of the resonant microwave frequency, the lumped element

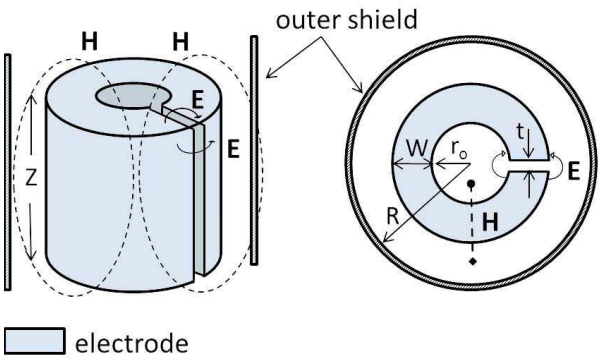

Fig. 3. Simplified sketch of a loop-gap resonator (n = 1) with the dimensions of interest.

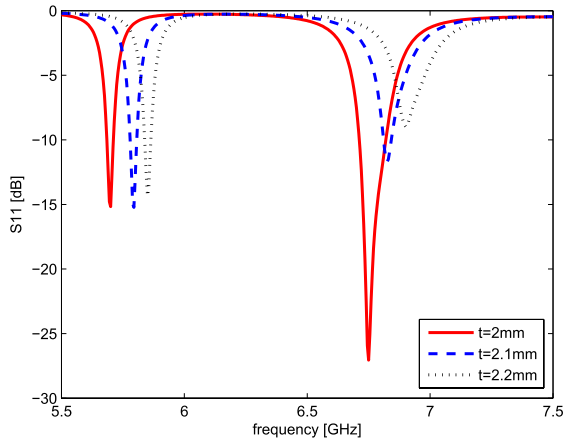

Fig. 4. Influence of gap size t on reflection coefficient. Resonance of interest is at 6.835 GHz (right), while the resonance at ~5.8 GHz (left) is a TM mode due to the size of the outer shield surrounding the μ-LGR.

model can be used and the electric and magnetic fields can be considered separated.

In a first order approximation represented by eq. 2, the resonance frequency f_r of the resonator is defined by the geometry of the electrode structure, including the radius (r_o), thickness (W), and length (Z) of the electrodes, and the width (t) and number (n) of gaps, as indicated in Fig. 3. Other versions of the formula, taking into account the fringing fields, the effect of the shield, and the limited length of the resonator can be found in [20]–[22].

$$C = \varepsilon \frac{WZ}{nt}, \quad L = \mu \frac{\pi r_o^2}{Z}$$
$$\rightarrow \quad f_r = \frac{1}{2\pi\sqrt{LC}} = \frac{1}{2\pi}\sqrt{\frac{n}{\pi r_o^2 \varepsilon \mu}\frac{t}{W}} \qquad (2)$$

A LGR can be coupled to external circuits both by capacitive or inductive means. In the first case a monopole probe is placed in proximity of the gap and interacts with the gap's fringe electric fields. In the latter case, an inductive loop can be used for coupling to the magnetic fields at either end of the resonator. In order to correct for inevitable manufacturing tolerances, fine tuning of the resonant frequency can be electronic [20] or mechanical [18], [23].

B. Model Validation

The resonator concept of operation was proven and optimized in several steps through software simulations, which aimed to study the influence of relevant geometrical features, as well as of the presence of the Rb cell and of the cavity apertures. In particular, the influence of gap size (t) and width of electrodes (W) were investigated in order to obtain the desired resonance frequency.

As an example, Fig. 4 shows the simulated reflection coefficient for three different values of the gap size. The resonance shifts to higher frequencies as both L and C decrease, while the matching (given by the minimum value of S_{11} close to 6.8GHz for our system) is also affected when t becomes too large. The influence of cavity apertures and dielectric properties of different materials were also investigated in order to determine a suitable design for manufacturing.

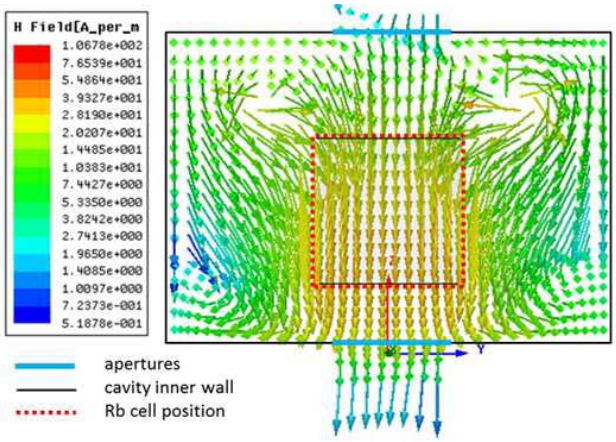

Fig. 5. Simulated magnetic field of the TE mode at 6.835GHz (t = 2.0mm). The position of the micro-fabricated Rb vapor cell is indicated by the red dotted line.

Finally, the influence of tuning screws was considered during the optimization of the electrodes structure, given their strong impact on both magnetic and electric fields. For $t = 2.0$ mm, the magnetic field at resonance has the desired TE mode distribution shown in Fig. 5, with a calculated FOF of $\xi \sim 0.8$.

IV. Resonator Design and Realization

The μ–LGR is composed of a multi-layered structure of conductive electrodes separated by cylindrical dielectric layers, stacked along axial direction (the z axis). These electrodes are two-dimensional structures, formed by patterns of metal film printed onto the dielectric layers. The dielectric material composing the resonator layers has a temperature-compensated dielectric constant in the microwave region. The electrodes are planar realizations of loop gap resonators, juxtaposed in pairs in order to obtain a series of stacked loop-gap electrodes with 2 gaps ($n = 2$) on each layer. The different layers of the electrode structure are electrically connected by means of metallized vias, but are not in electrical contact with the outer metal enclosure. A photograph of the assembled electrode stack surrounding the Rb cell is shown in Fig. 2c.

Fig. 6. Some of the built prototypes based on the μ-LGR optimized solution.

Coupling of the microwave excitation to the μ-LGR is achieved by a loop-shaped strip-line, printed onto a separate layer of dielectric material. This excitation loop is placed above the μ-LGR electrode stack and is fed by a coaxial line. In the present realization, a cylindrical brass box encloses the multi-layer resonator structure, the coupling device and the Rb cell, to form an electrically conducting outer shield. This shield is in contact with the outer jacket of the coaxial line and is positioned relative to the other parts of the μ-LGR by means of dielectric spacing washers of appropriate size. The shield has apertures at its ends to allow the laser beam to interact with the Rb atomic vapor, which is held in a micro-fabricated cell [16] placed in the center of the μ-LGR. A temperature stabilized substrate was selected [24], in order to ensure the stability of the relative dielectric primitivity with temperature. Thus, the resonant frequency of the resonator remains constant over temperature [25]. Two screws mounted into the outer shield and protruding into the μ-LGR allow the fine tuning of the resonant frequency. The proposed technology allows for fully demounting the μ-LGR, in case the Rb cell or other parts of the resonator need to be removed or changed. A photograph of the fully assembled μ-LGR with its brass shield is shown in Fig. 2(b).

V. Experimental Evaluation

A. Measurements and Simulations

Several prototypes based on the μ-LGR optimized solution were built, as shown in Fig. 6. Considering the influence of the gap width t on resonance frequency, the prototypes present different values of t (from 1.9 to 2.3 mm, with a step of 0.1 mm). The built resonators were measured and tuned using a vector network analyzer (VNA, Agilent 8720D). The magnitude of the reflection coefficient $|S_{11}|$ at the coaxial cable port was monitored during the tuning process. In Fig. 7(a) the simulated model of one of the prototypes ($t = 2.0$ mm) is compared to the equivalent measured resonator. Results show good agreement and the small frequency shift is due to fabrication and assembly tolerances. The loaded quality factor Q_L is $\approx$26. This relatively low Q-factor does not limit the atomic clock performance, and is in fact rather helpful for its achievable stability, as discussed in section VI-D.

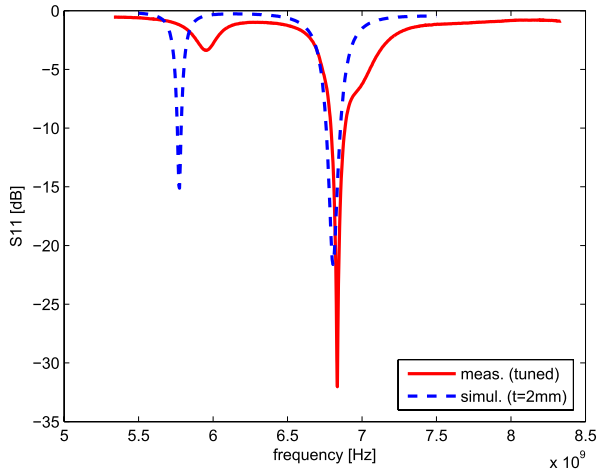

(a)

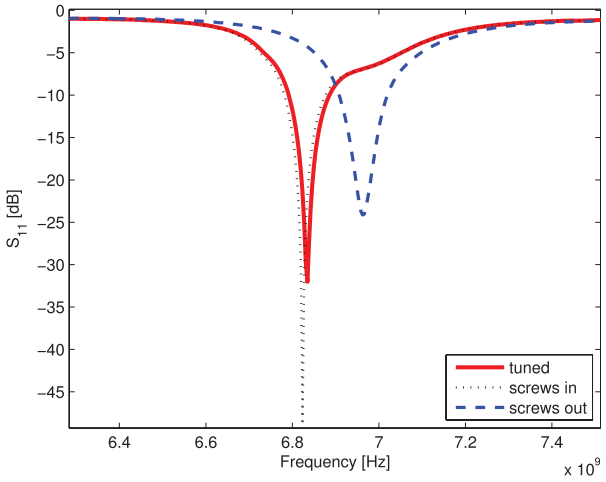

(b)

Fig. 7. (a) Comparison between the reflection coefficient of one measured prototype ($t = 2.0$ mm, tuned) and model simulation for $t = 2.0$ mm with maximum insertion of the two screws. The resonance frequency f_r is slightly higher in the measured prototype due to fabrication and assembly tolerances. (b) Measured frequency tuning of the μ-LGR prototype ($t = 2.0$ mm) around 6.835 GHz, for different positions of the tuning screws.

B. Fine Tuning of the Resonance Frequency

The two tuning screws proved to be an efficient means to achieve the desired Rb resonance frequency at 6.835 GHz. The average tuning capability Δ_t is 140 MHz for the built prototypes. The tuning of one prototype ($t = 2.0$ mm) is shown in Fig. 7(b). A comparison of the results obtained by simulations and measurements on prototypes using different values of t is given in Table I.

C. Frequency Tuning With Temperature

The influence of temperature on the resonance frequency f_r of the μ-LGR cavity was investigated by placing the μ-LGR in a temperature-controlled enclosure and measuring the $|S_{11}|$ parameter as function of microwave frequency for different μ-LGR temperatures (see Fig. 8). The heating of the

TABLE I

RESONANCE FREQUENCY f_r OF THE μ-LGR: COMPARISON BETWEEN HFSS SIMULATIONS AND MEASURED PROTOTYPES. Q_L VALUES ARE CALCULATED FROM EXPERIMENTALLY MEASURED DATA SIMILAR TO THOSE SHOWN IN FIG. 7B.

	f_r screws in [GHz]		f_r screws out [GHz]			
Prototype	HFSS	Meas.	HFSS	Meas.	Δ_t [MHz]	Q_L
$t = 1.9$	6.700	6.778	6.815	6.891	113	30
$t = 2.0$	6.715	6.811	6.805	6.943	132	26
$t = 2.1$	6.745	6.824	6.830	7.016	192	23
$t = 2.2$	6.770	6.815	6.860	6.937	122	26
$t = 2.3$	6.785	6.830	6.910	6.975	145	26

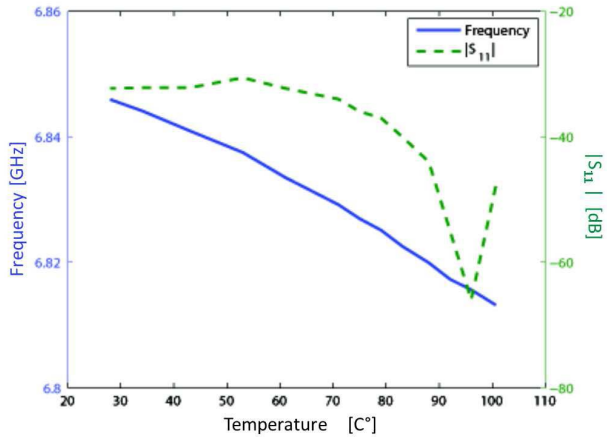

Fig. 8. Measured dependence of resonator temperature on μ-LGR resonance center frequency and $|S_{11}|$, between 20°C and 100°C.

cavity was realized with a resistive wire and the temperature was recorded with NTC sensors. The cavity properties were studied in a temperature range covering 20°C to 100°C, in order to evaluate their impact on the performance of the atomic clock at the operation temperature of ≈80 °C. Results show a maximum frequency shift of about 30 MHz over the entire temperature range studied, which can be easily corrected for using the tuning screws. Note that the frequency shift of the atomic clock output will be mainly governed by the atomic signal, and thus its variation with temperature will be much lower than that of the μ-LGR frequency shown here (see also Fig. 13). The reflection coefficient at resonance remains below −30 dB for all temperatures, as shown in Fig. 8.

VI. SPECTROSCOPY RESULTS

In this section, we report on double-resonance (DR) spectroscopic studies using the μ-LGR described above, and its implementation for operation of a DR Rb atomic clock.

A. Experimental Setup

A DR experiment consists of measuring the resonance spectrum of the ground state magnetic dipole transitions of a population of rubidium atoms in vapor phase (held inside the vapor cell), polarized through optical pumping [26]. The resonant magnetic field applied to the atoms is sustained by the MWR cavity, while the resonant optical field is generated by a frequency stabilized laser head [27], in this case using a distributed-feed-back laser diode emitting on the Rb D2 line at

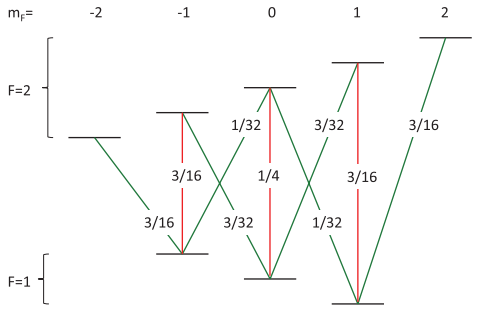

Fig. 9. Microwave transition probabilities in terms of theoretical values for $|\langle k|S_z|j\rangle|^2$ (π transitions, red vertical lines) and $|\langle k|S_x|j\rangle|^2$ (σ transitions, green diagonal lines) for the ^{87}Rb $5^2S_{1/2}$ ground state.

780 nm [28]. In order to verify the suitability of the proposed solution, the μ-LGR loaded with the vapor cell was integrated in an experimental Double Resonance (DR) setup (see Fig. 1). A dedicated mounting support was fabricated to receive the μ-LGR for evaluation, consisting of a temperature regulated aluminium enclosure surrounded by a solenoid for applying the dc magnetic field, required to create the quantization axis and isolate the $|F_g = 1; m_F = 0\rangle \rightarrow |F_g = 2; m_F = 0\rangle$ clock transition by Zeeman splitting. The whole is surrounded by a μ-metal shield, used to suppress external magnetic field fluctuation that would eventually perturb the atomic levels, and is finally held within a foam support for thermal isolation. The μ-LGR is driven at the desired frequency by a laboratory RF synthesizer. This spectroscopic setup can be transformed into an atomic clock using a synchronous detection scheme and sending the error signal for the microwave frequency via a proportional/integrator controller to the EFC (electronic frequency control) input of the synthesizer.

B. Double-Resonance Signal

In the vicinity of the atomic transition frequency ν_0, the magnetic dipole transition probability between two atomic states can be expressed as [1]:

$$P_{k'k} = \frac{\pi |W_{kk'}|^2}{2\hbar^2} g(\nu - \nu_0) \tag{3}$$

with the transition matrix elements

$$W_{kk'} = \langle F = 2, k|\vec{\mu} \cdot \vec{B}|F = 1, k'\rangle = \begin{cases} \langle k|S_z|k'\rangle \mu_B g_J B_\parallel & \text{for } \pi \text{ transitions} \\ \langle k|S_x|k'\rangle \mu_B g_J B_\perp & \text{for } \sigma \text{ transitions} \end{cases} \tag{4}$$

where $g(\nu - \nu_0)$ represents the spread of the resonance frequency for the considered transition due to the finite lifetime of the atoms, and ν_0 depends on the local strength of the applied C-field. $B_\parallel$ and $B_\perp$ are the components of the RF magnetic field parallel and orthogonal, respectively, to the local C-field (oriented along the z-axis). S is the spin angular momentum operator and k, k' are associated to the m_F quantum numbers of the S-wave ground states of the ^{87}Rb. The π, σ^+, and σ^- transitions here denote transitions that change the atomic m_F quantum number by $\Delta m_F = m_F (F = 2) - m_F (F = 1) = 0, +1$, and -1, respectively. Figure 9 shows a sketch of all allowed magnetic dipole transitions and

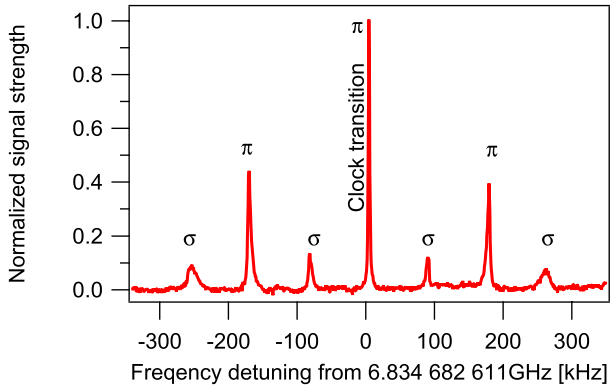

Fig. 10. DR spectrum of the clock transition and all Zeeman lines, measured using the μ-LGR.

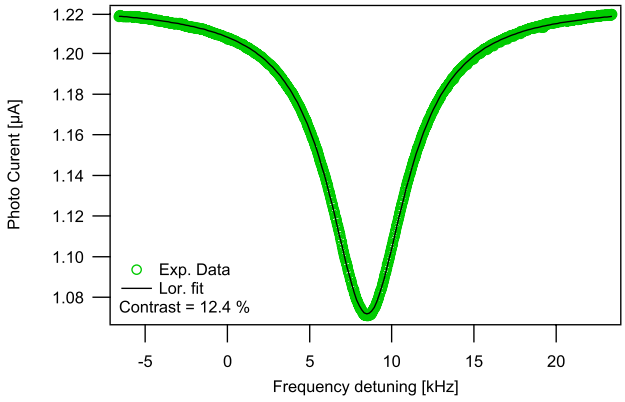

Fig. 11. DR signal of the clock transition, measured with the μ-LGR in conditions for optimized clock short-term stability. The signal has a contrast of 12.4% and a linewidth of 5.8 kHz.

their respective unnormalized weights. It is interesting to note that $\sum_\pi |\langle k|S_z|j\rangle|^2 = \sum_\sigma |\langle k|S_x|j\rangle|^2$ showing that neither the σ nor π transitions are intrinsically favoured, thus only the direction of the RF magnetic field compared to the C-field weights these transitions. The strength S of the DR lines shown in Figure 10 is a direct measure of these transition probabilities integrated over the whole cell volume [17], therefore:

$$\xi_{\text{exp}} = \frac{\int dv S_\pi}{\int dv S_\pi + \int dv S_\sigma} = \frac{\int dV |B_\parallel|^2}{\int dV |B_\parallel|^2 + \int dV |B_\perp|^2} \quad (5)$$

can be used as an experimental measure for the FOF defined in Equation 1. From our spectroscopic data, we find an experimental value of $\xi_{\text{exp}} = 0.7$ for the FOF of the μ-LGR, which is close to the FOF of $\xi_{\text{sim}} = 0.8$ found from the numerical simulations. Remaining discrepancies may be attributed to residual inhomogeneities in the dc magnetic field or beginning microwave saturation on the π transitions.

C. Clock Signal and Frequency Instability

Figure 11 shows a close zoom onto the clock transition, after optimization of the interrogation parameters; cavity and cell temperature were stabilized at 90°C, the laser frequency was locked to the $F_g = 1 \rightarrow F_e = \{0, 1\}$ cross-over optical transition using the Doppler-free saturated-absorption spectroscopy setup within the laser head [27], [29]. The laser

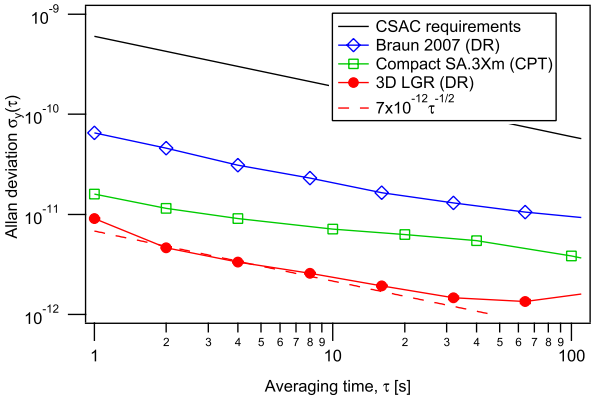

Fig. 12. Clock frequency instability measured with the μ-LGR (filled red bullets), compared to the stabilities of a commercially available clock based on coherent population trapping (CPT, open green squares) [30], and the miniature DR-based clock of reference (open blue diamonds) [10]. The solid black line gives the performance goal for the DARPA CSAC project [9].

intensity incident on the μ-LGR was 9.25 μW/mm^2 and the RF input power to the μ-LGR was set to -10 dBm. From the signal properties, such as linewidth and amplitude, we predict a short-term clock instability of $\sigma_y(\tau) = 6.6 \times 10^{-12}\tau^{-1/2}$, using the formula:

$$\sigma_y(\tau) = \frac{N}{\sqrt{2} \cdot \nu_0 \cdot A/\Gamma}\, \tau^{-1/2} \quad (6)$$

where N is the total detector noise, Γ the signal linewidth, A the amplitude and ν_0 the frequency of the microwave transition. Figure 12 shows the measured clock short-term frequency instability obtained by stabilizing the synthesizer's internal quartz oscillator to the clock transition (see Fig. 11). The measured clock instability is $7 \times 10^{-12}\tau^{-1/2}$, in good agreement with the predicted value. This excellent short-term instability, well below $1\times10^{-11}\tau^{-1/2}$, proves the suitability of the μ-LGR for DR-based miniature atomic clocks with state-of-the-art clock stabilities.

D. Impact of Temperature Sensitivity on the Clock

The temperature dependence of the μ-LGR resonance frequency of the cavity is ≈0.4 MHz/K (see section V-C) and might not be compatible with the desired clock stability of few mHz (10^{-13} level) at longer averaging times. Fortunately, the relatively low quality factor strongly reduces the impact of a cavity resonance frequency offset on the atomic resonance frequency ("cavity pulling"). In passive rubidium frequency standards, the induced offset of the atomic resonance can be expressed as [1]:

$$\Delta\nu_{\text{clock}} \approx 3 \times 10^{-3}\, \frac{Q_L}{Q_a}\, \Delta\nu_{\text{cavity}} \quad (7)$$

where Q_L and Q_a are the quality factor of the loaded cavity and of the atomic transition, respectively, and $\Delta\nu_{\text{cavity}}$ is the offset of the cavity resonance frequency from the atomic resonance frequency. For the μ-LGR the temperature sensitivity of the cavity resonance thus results in a temperature coefficient of the clock transition due to cavity pulling of only 4.3×10^{-12} K^{-1}. This is more than two orders of magnitude

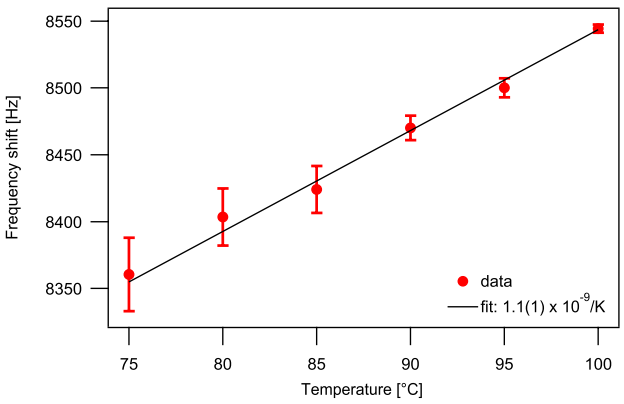

Fig. 13. Measured temperature shift of the clock frequency, dominated by buffer-gas effects in the micro-fabricated cell.

lower than the experimentally measured temperature sensitivity of the clock transition (see Fig. 13) that is dominated by the temperature shift introduced by the non-optimized buffer-gas mixture used in the cell [31]. The temperature dependence of the μ-LGR frequency reported in Fig. 8 thus does not impose limitations to the achievable clock stability here. With the temperature of the μ-LGR controlled within 10 mK at averaging times $\tau \geq 10^3$s, the maximal relative frequency fluctuation arising from this temperature sensitivity is 4.3×10^{-14}, which is sufficiently small for any miniature atomic clock currently envisaged.

VII. Conclusion

We have presented and analyzed the μ-LGR, a novel type of miniaturized microwave resonator for miniature atomic clock applications. The concept of the proposed device was validated and optimized through software simulations studying the influence of relevant geometrical features, the presence of the Rb cell inside the μ-LGR and of the cavity apertures. Experimental results obtained on prototypes of the μ-LGR are in agreement with simulated results, showing that the prototypes could be easily tuned to the desired Rb resonance frequency of 6.835 GHz. Temperature-induced shifts of the resonator resonance frequency were measured and can be corrected for by using the tuning screws.

For the presented prototypes, the outer dimensions of the MWR are significantly increased by the brass outer shield used for first demonstration of the μ-LGR principle. The overall volume of the μ-LGR is therefore expected to be reduced in the future by using a simplified and more compact shield. Analysis of the temperature-dependent frequency shifts for the μ-LGR and the overall DR clock shows that the temperature sensitivity of the μ-LGR is not limiting for the achievable medium- to long-term clock stability.

The spectroscopic evaluation results show that the μ-LGR is well-suited for the realization of a new class of miniature DR atomic clocks, that can achieve excellent frequency stabilities of $7 \times 10^{-12}\tau^{-1/2}$ as demonstrated by our clock stability measurement using the μ-LGR. Such frequency standards are of high interest for applications of chip-scale atomic clocks as well as of highly compact Rb clocks with improved stabilities, for example in network synchronization or smart grids.

Acknowledgment

The authors would like to thank Y. Pétremand (EPFL-SAMLAB, now with CSEM Centre Suisse d'Electronique et de Microtechnique SA, Neuchâtel, Switzerland) for manufacturing the miniature Rb cell, P. Scherler (UniNe-LTF) for experimental assistance, and A. Horsley (Universität Basel, Switzerland) for proof-reading the manuscript.

References

[1] J. Vanier and C. Audoin, *The Quantum Physics of Atomic Frequency Standards*. Bristol, U.K.: A. Hilger, 1989.
[2] J. Camparo, "The rubidium atomic clock and basic research," *Phys. Today*, vol. 60, no. 11, pp. 33–39, Nov. 2007.
[3] J. A. Kusters and C. A. Adams, "Performance requirements of communication base station time standards," *RF Design*, vol. 22 pp. 28–38, May 1999.
[4] L. A. Mallette, P. Rochat, and J. White, "Historical review of atomic frequency standards used in space systems," in *Proc. 38th Precise Time and Time Interval Meeting, PTTI*, Washington, DC, USA, Dec. 2006.
[5] S. Knappe, "MEMS atomic clocks," in *Comprehensive Microsystems*, vol. 3. Amsterdam, The Netherlands: Elsevier, 2008.
[6] *SA.45s CSAC Chip Scale Atomic Clock Datasheet*, document DS/SA.45s CSAC/123010/pdf, Symmetricom Inc., San Jose CA, USA, 2010.
[7] M. A. Lombardi, "Microsecond accuracy at multiple sites: Is it possible without GPS?" *IEEE Instrum. Meas. Mag.*, vol. 15, no. 5, pp. 14–21, Oct. 2012.
[8] M. Pellaton, C. Affolderbach, Y. Pétremand, N. de Rooij, and G. Mileti, "Study of laser-pumped double-resonance clock signals using a micro-fabricated cell," *Phys. Scripta*, vol. 2012, no. T149, p. 014013, 2012.
[9] R. Lutwak, D. Emmons, W. Riley, and R. M. Garvey, "The chip-scale atomic clock-coherent population trapping vs. conventional interrogation," in *Proc. 34th Annu. PTTI Meeting*, Dec. 2002, pp. 539–550.
[10] A. M. Braun *et al.*, "RF-interrogated end-state chip-scale atomic clock," in *Proc. 39th Annu. Precise Time and Time Interval Meeting, PTTI*, Nov. 2007, pp. 233–248.
[11] H. Schweda, G. Busca, and P. Rochat, "Atomic frequency standard," E.P. Patent 0 561 261, Jul. 1997.
[12] J. Deng, "Subminiature microwave cavity for atomic frequency standards," in *Proc. IEEE Int. Freq. Control Symp. PDA Exhibit.*, Jun. 2001, pp. 85–88.
[13] B. Xia, D. Zhong, S. An, and G. Mei, "Characteristics of a novel kind of miniaturized cavity-cell assembly for rubidium frequency standards," *IEEE Trans. Instrum. Meas.*, vol. 55, no. 3, pp. 1000–1005, Jun. 2006.
[14] M. Violetti, C. Affolderbach, F. Merli, G. Mileti, and A. K. Skrivervik, "Microwave resonator, quantum sensor, and atomic clock," E.P. Patent 12 155 696, Feb. 16, 2012.
[15] M. Violetti *et al.*, "New miniaturized microwave cavity for rubidium atomic clocks," in *Proc. IEEE Sensors Conf.*, Taipei, Taiwan, Oct. 2012, pp. 315–318.
[16] Y. Pétremand *et al.*, "Microfabricated rubidium vapour cell with a thick glass core for small-scale atomic clock applications," *J. Micromech. Microeng.*, vol. 22, no. 2, p. 025013, 2012.
[17] C. Stefanucci *et al.*, "Compact microwave cavity for high performance rubidium frequency standards," *Rev. Sci. Instrum.*, vol. 83, no. 10, p. 104706, 2012.
[18] W. N. Hardy and L. A. Whitehead, "Split-ring resonator for use in magnetic resonance from 200–2000 MHz," *Rev. Sci. Instrum.*, vol. 52, no. 2, pp. 213–216, Feb. 1981.
[19] T. Sphicopoulos and F. Gardiol, "Slotted tube cavity: A compact resonator with empty core," *IEE Proc. H, Microw., Antennas Propag.*, vol. 134, no. 5, pp. 405–410, Oct. 1987.
[20] M. Mehdizadeh, T. K. Ishii, J. S. Hyde, and W. Froncisz, "Loop-gap resonator: A lumped mode microwave resonant structure," *IEEE Trans. Microw. Theory Techn.*, vol. 31, no. 12, pp. 1059–1064, Dec. 1983.
[21] M. Mehdizadeh and T. Ishii, "Electromagnetic field analysis and calculation of the resonance characteristics of the loop-gap resonator," *IEEE Trans. Microw. Theory Techn.*, vol. 37, no. 7, pp. 1113–1118, Jul. 1989.
[22] W. Froncisz and J. S. Hyde, "The loop-gap resonator: A new microwave lumped circuit ESR sample structure," *J. Magn. Reson.*, vol. 47, no. 3, pp. 515–521, 1982.
[23] G. Mei, D. Zhong, S. An, J. Liu, and X. Huang, "Miniaturized microwave cavity for atomic frequency standard," U.S. Patent 6 225 870 B1, May 1, 2001.

[24] Rogers Corporation, "A temperature microwave laminate for microastrip patch antenna applications," *Microw. J.*, vol. 37, no. 11, pp. 130–131, Nov. 1994.
[25] J.-F. Zürcher, "On some thermal properties of microstrip antennas," *Microw. Opt. Technol. Lett.*, vol. 10, no. 5, pp. 261–263, 1995.
[26] J. Vanier and C. Mandache, "The passive optically pumped Rb frequency standard: The laser approach," *Appl. Phys. B*, vol. 87, no. 4, pp. 565–593, 2007.
[27] C. Affolderbach and G. Mileti, "A compact laser head with high-frequency stability for Rb atomic clocks and optical instrumentation," *Rev. Sci. Instrum.*, vol. 76, no. 7, p. 073108, 2005.
[28] F. Gruet, M. Pellaton, C. Affolderbach, T. Bandi, R. Matthey, and G. Mileti, "Compact and frequency stabilized laser heads for rubidium atomic clocks," in *Proc. Int. Conf. Space Opt., ICSO*, Corsica, France, Oct. 2012.
[29] D. W. Preston, "Doppler-free saturated absorption: Laser spectroscopy," *Amer. J. Phys.*, vol. 64, no. 11, pp. 1432–1436, 1996.
[30] J. Deng, P. Vlitas, D. Taylor, L. Perletz, and R. Lutwak, "A commercial CPT rubidium clock," in *Proc. 22nd EFTF*, Toulouse, France, 2008, no. FPE–0099.
[31] J. Vanier, R. Kunski, N. Cyr, J. Savard, and M. Tetu, "On hyperfine frequency shifts caused by buffer gases: Application to the optically pumped passive rubidium frequency standard," *J. Appl. Phys.*, vol. 53, no. 8, pp. 5387–5391, 1982.

Maddalena Violetti was born in Siena, Italy, in 1981. She received the Laurea degree in telecommunications engineering from the University of Siena, Siena, in 2007, and the Ph.D. degree in electrical engineering from École Polytechnique Fédérale de Lausanne, Lausanne, Switzerland, in 2012. She is currently a Research Associate with the University of Siena, where she is involved in projects funded by the European Space Agency and the European Union in the field of applied electromagnetics. Her research interests include small antenna-based sensors for industrial applications and metamaterial-based devices for antenna pattern shaping and polarization control.

Matthieu Pellaton was born in Basel, Switzerland, in 1984. He received the B.Sc. and M.Sc. degrees in physics from the University of Neuchâtel, Neuchâtel, Switzerland, in 2008 and 2009, respectively, where he is currently pursuing the Ph.D. degree at the Laboratoire Temps - Fréquence. In 2012, he did a summer internship at the European Space Research and Technology Centre, Noordwijk, The Netherlands. His major research interests include atomic spectroscopy, vapour cell fabrication, and miniature frequency standards.

Christoph Affolderbach (M'13) received the Diploma and Ph.D. degrees in physics from the University of Bonn, Bonn, Germany, in 1999 and 2002, respectively.

He has been a Research Scientist with the Observatoire Cantonal de Neuchâtel, Neuchâtel, Switzerland, from 2001 to 2006. In 2007, he joined the Laboratoire Temps-Fréquence, University of Neuchâtel, Neuchâtel, as a Scientific Collaborator. His research interests include the development of stabilized diode laser systems, atomic spectroscopy, and vapor-cell atomic frequency standards, in particular, laser-pumped high-performance atomic clocks and miniaturized frequency standards.

Dr. Affolderbach is member of the German Physical Society and the Swiss Physical Society.

Francesco Merli (M'07) received the Laurea (*cum laude*) degree in telecommunication engineering from the University of Florence, Florence, Italy, in 2006, and the Ph.D. degree in electrical engineering from Ecole Polytechnique Fédérale de Lausanne, Lausanne, Switzerland, in 2011. He is currently with Huber & Suhner AG, Herisau, Switzerland. His research interests include antenna theory with particular focus on implantable and ultrawideband antennas, spherical wave analysis, biomedical applications, wireless sensing, and atomic watch cavities.

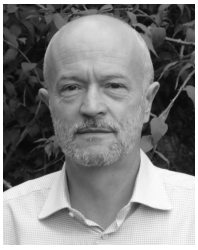

Jean-François Zürcher was born in Vevey, Switzerland, in 1951. He received the degree in electrical engineering from Ecole Polytechnique Fédérale de Lausanne (EPFL), Lausanne, Switzerland, in 1974. He is currently a Scientific Associate with the Laboratoire d'Electromagnétisme et d'Acoustique at EPFL, where he is the Manager of the Microwave Laboratory. His main interest lies in the domain of microstrip circuits and antennas. In 1988, he invented the Strip Slot Foam Inverted Patch antenna, which became a commercial product. He is currently developing instrumentation and techniques for the measurement of near fields of planar structures and microwave materials measurement and imaging. He has authored and co-authored about 180 publications, chapters in books, and papers presented at international conferences. He has co-authored the book *Broadband Patch Antennas* (Artech House, 1995), and holds nine patents.

Gaetano Mileti received the Engineering degree in physics from Ecole Polytechnique Fédérale de Lausanne, Lausanne, Switzerland, in 1990, and the Ph.D. degree in physics from the University of Neuchâtel, Neuchâtel, Switzerland, in 1995. From 1991 to 1995, and from 1997 to 2006, he was a Research Scientist with the Observatoire Cantonal de Neuchâtel. From 1995 to 1997, he was with the National Institute of Standards and Technology, Boulder, CO, USA. In 2007, he co-founded the Laboratoire Temps - Fréquence at the University of Neuchâtel, where he is the Deputy Director and an Associate Professor. His research interests include atomic spectroscopy, stabilized lasers, and frequency standards.

Anja K. Skrivervik received the Degree in electrical engineering and the Ph.D. degree from Ecole Polytechnique Fédérale de Lausanne (EPFL), Lausanne, Switzerland, in 1986 and 1992, respectively, for which she received the Latsis Award. After a stay at the University of Rennes, Rennes, France, as an invited Research Fellow and two years in the industry, she returned part time to EPFL as an Assistant Professor in 1996, where she is currently a Professeur Titulaire. Her teaching activities include courses on microwaves and antennas. Her research activities include electrically small antennas, implantable and wearable antennas, multifrequency and ultrawideband antennas, numerical techniques for electromagnetics, and microwave and millimeter-wave MEMS. She has authored and co-authored more than 200 scientific publications, and holds five patents. She is very active in the European collaboration and the European projects. She was the Chairperson of the Swiss URSI until 2012, a Board Member of the European School on Antennas, and a Board Member of the Center for High Speed Wireless Communications of the Swedish Foundation for Strategic Research.